Acta Neuropathol (2002) 104:525–533
DOI 10.1007/s00401-002-0585-x

REGULAR PAPER

**Annemieke A. M. Rensink · Henkjan Gellekink
Irene Otte-Höller · Hans J. ten Donkelaar
Robert M. W. de Waal · Marcel M. Verbeek
Berry Kremer**

Expression of the cytokine leukemia inhibitory factor and pro-apoptotic insulin-like growth factor binding protein-3 in Alzheimer's disease

Received: 17 January 2001 / Revised: 11 April 2002 / Accepted: 16 May 2002 / Published online: 20 July 2002

Abstract Amyloid-β (Aβ) deposition in cerebral blood vessel walls is one of the key features of Alzheimer's disease (AD). $A\beta_{1–40}$ carrying the "Dutch" mutation ($DA\beta_{1–40}$) induces rapid degeneration of cultured human brain pericytes (HBP). To study the mechanisms of this Aβ-induced toxicity, a comparative cDNA expression array was performed to detect differential gene expression of Aβ-treated versus untreated HBP. Messenger RNA expression of leukemia inhibitory factor (LIF) and insulin-like growth factor binding protein 3 (IGFBP-3) was increased in $DA\beta_{1–40}$-treated HBP, whereas early growth response factor-1 (Egr-1) expression was decreased. Corresponding protein expression was investigated in AD and control brains. In all AD cases examined, LIF expression was observed in senile plaques and cerebral amyloid angiopathy, whereas IGFBP-3 expression in these lesions was only observed in a subset of cases. LIF and IGFBP-3 were also expressed in neurofibrillary tangles, as well as in neurons in AD and control brains. Egr-1 was predominantly expressed in astrocytes. Given its known involvement in both neuronal and immune responses to injury, the cytokine LIF may be a mediator of the inflammatory reaction seen in AD. IGFBP-3 is known to inhibit cell proliferation and induce apoptosis and may therefore contribute to neuronal degeneration in AD.

Keywords Alzheimer's disease · Amyloidβ · Leukemia inhibitory factor · Insulin-like growth factor binding protein-3 · Inflammation

A.A.M. Rensink · H. Gellekink · H.J. ten Donkelaar
M.M. Verbeek · B. Kremer
Departments of Neurology, University Medical Center, Nijmegen, The Netherlands

A.A.M. Rensink (✉) · H. Gellekink · I. Otte-Höller
R.M.W. de Waal
437, Department of Pathology,
University Medical Center Nijmegen,
P.O. Box 9101, 6500 HB Nijmegen, The Netherlands
e-mail: a.rensink@pathol.azn.nl,
Tel.: +31-2436-18897/14326, Fax: +31-2435-40520

Introduction

Senile plaques (SPs) and cerebral amyloid angiopathy (CAA) are two of the key pathological lesions of Alzheimer's disease (AD). The major component of these lesions is the 39–42 amino acid amyloid β protein (Aβ) [11], which is proteolytically cleaved from the larger amyloid β precursor protein (APP). CAA is also a characteristic of the autosomal dominant disorder hereditary cerebral hemorrhage with amyloidosis-Dutch type (HCHWA-D). HCHWA-D is caused by a mutation at amino acid 22 of the Aβ sequence [18], resulting in extensive amyloid deposition in the small leptomeningeal arteries and cortical arterioles, often leading to fatal hemorrhages.

Amyloid deposition in vessels causes degeneration of human brain pericytes (HBP) and smooth muscle cells (SMC) (i.e., cerebrovascular cells) [13, 35], while deposition of Aβ in SPs is associated with neuronal degeneration [16]. Previously, we have established a cell culture model using HBP to investigate the cellular toxicity of Aβ. Synthetic $A\beta_{1–42}$ peptide, but not $A\beta_{1–40}$, caused degeneration of cultured HBP [31, 33] and $A\beta_{1–40}$ containing the "Dutch" mutation ($DA\beta_{1–40}$) induced an even more pronounced degeneration of HBP and SMC [6]. Moreover, only soluble, non-aggregated Aβ peptides are toxic to cerebrovascular cells [7, 31, 32]. The soluble pathogenic forms of Aβ assemble into an elaborate network of fibrils on the SMC surface [29], prior to an increase in cell-associated APP and subsequent cellular degeneration [19]. However, the precise pathogenic mechanism of Aβ-induced toxicity remains unclear. Thus, identification of the mediators of Aβ-induced cell death is of great importance to unravel pathways leading to Aβ-induced toxicity.

In the present study, we used the in vitro model of Aβ-mediated toxicity in HBP to identify potential effector molecules. Hereto, differential gene expression analysis was used to compare the expression level of a selected number of genes in $DA\beta_{1–40}$-treated versus untreated HBP. Several genes, 25 in total, were found to be differentially expressed. Leukemia inhibitory factor (LIF), insulin-like growth factor (IGF) binding protein 3 (IGFBP-3)

and early growth response factor 1 (Egr-1) were selected for further investigation, because of the clear difference in mRNA expression levels, their involvement in cell survival and cell death, and because of the availability of an antibody for immunohistochemistry. Differential expression was investigated at the protein level in cultured HBP either treated or not with $DA\beta_{1–40}$. Moreover, protein expression patterns of these genes were examined by immunohistochemical staining in the cerebral cortex and hippocampus of AD and control patients.

Materials and methods

Materials

Synthetic $DA\beta_{1–40}$, 89% pure, was obtained from Biosource (Etten-Leur, The Netherlands). This peptide contains a glutamine instead of a glutamic acid residue at position 22. Lyophilized peptide was dissolved in sterile water at 250 µM and stored at –80°C prior to use. All primary antibodies and their sources are listed in Table 1. All biotin-labeled secondary antibodies, the avidin-biotin-peroxidase complex (ABC) and sheep anti-mouse-fluorescein isothiocyanate (FITC) were obtained from Vector Laboratories (Burlingame, Calif.). Swine anti-rabbit-FITC and sheep anti-mouse-peroxidase were purchased from DAKO Corporation (Carpinteria, Calif.) and Donkey anti-goat-peroxidase was purchased from Jackson Immunoresearch Laboratories (Pa.).

Cell culture

HBP were isolated and characterized as described previously [30]. Cells were maintained in Eagle's modification of essential medium (EMEM, Bio-Whittaker, Verviers, Belgium) supplemented with 10% human serum, 20% newborn calf serum, 1 ng/ml basic fibroblast growth factor and antibiotics. For comparative cDNA microarray analysis, cells were cultured in a culture flask and for all other experiments in eight-well chamber slides (Nunc, Roskilde, Denmark). Prior to experiments, cells were incubated in EMEM containing 0.1% bovine serum albumin (BSA) and antibiotics for at least 4 h. Subsequently, cells were incubated in fresh EMEM/0.1%BSA, either supplemented or not with synthetic $DA\beta_{1–40}$ peptide at 25 µM, for the indicated number of days.

Comparative cDNA microarray analysis

cDNA microarray analysis was performed using the Atlas human cDNA Expression Array (Clontech Laboratories, Calif.) according to the instructions of the manufacturer, with few alterations described below.

This array consists of 588 human cDNAs (representing genes of different functional classes, including transcription factors, cytokines, oncogenes and tumor suppressor genes), 9 housekeeping control cDNAs and negative controls, all immobilized in duplicate dots on a nylon membrane. [α-^{32}P]dCTP-labeled cDNAs were prepared from total RNA of $DA\beta_{1–40}$-treated and untreated HBP. These two cDNA pools were used to hybridize two identical arrays. The entire experiment, beginning with treatment of HBP with $DA\beta_{1–40}$, was performed in duplicate.

After a 3-day incubation, total RNA was isolated from HBP either treated or not with Aβ using the RNAzol B protocol (Campro Scientific, Veenendaal, The Netherlands). After isolation, the RNA pellet was resuspended in 20 µl DEPC-treated water for 30 min at 56°C and stored at –80°C prior to use. Of the total RNA, 20 µg was treated with RNase-free DNase I (Boehringer Ingelheim, Germany, 1 U/µg RNA) at 37°C for 1 h in an air incubator in a total volume of 50 µl, to remove possible genomic DNA contamination. Subsequently, the RNA sample was purified using phenol:chloroform (1:1) and precipitated with NH_4OAc and ethanol. The precipitate was dissolved in 5 µl of deionized water to a final RNA concentration of 2–5 µg/µl and then 5 µg of total RNA was converted into a [α-^{32}P]dCTP-labeled first-strand cDNA probe. Chromaspin-200 DEPC-H_2O columns were used to separate non-incorporated label from the probe. The entire pool of labeled cDNA probe was mixed with a denaturing solution (1 M NaOH, 10 mM EDTA) and incubated for 20 min at 68°C. Then, Cot-1 DNA (to capture non-specific DNA) and neutralizing solution (1 M NaH_2PO_4, pH 7.0) was added and the incubation at 68°C was continued for 10 min. This mixture was added to 5 ml of the prehybridization solution containing a final radiolabel concentration of approximately 0.5×10^6–2×10^6 cpm/ml. After prehybridization with denatured sheared salmon testis DNA (to avoid nonspecific binding of the probe), the Atlas Array was incubated overnight with the hybridization mixture with continuous agitation at 68°C. Subsequently, the Atlas Array was washed twice in 200 ml wash solution 1 (2× SSC, 1% SDS) for 30 min with continuous agitation at 68°C, followed by an additional 30-min wash in 200 ml wash solution 2 (0.1× SSC, 0.1% SDS) with continuous agitation at 68°C. The damp membrane was immediately wrapped in plastic and exposed to a Kodak BioMax MS film at –70°C with an intensifying screen for different time periods. All mixtures, buffers (except washing buffers) and spin columns were provided by Clontech Laboratories.

Autopsy material

Brain tissue from patients with clinically diagnosed and neuropathologically confirmed AD and from controls (without neurological disease) was obtained from autopsy material. A definite diagnosis of AD was based on a combination of neuropathological [21] and clinical criteria. Tissue samples from frontal or temporal cortex and hippocampus were obtained from 5 control patients [4 female, 1 male; age 74.0±8.0 years; post-mortem delay (PMD) 4.6±1.3 h] and 13 AD patients (8 female, 5 male; age 79.6±8.0 years; PMD 4.4±2.0 h). Tissue samples were frozen in liquid nitrogen immediately after removal and stored at –80°C.

Immunohistochemical staining of human brain cryosections

Air-dried sections from frozen tissue (5 µm thick) were fixed in acetone for 10 min and preincubated for 30 min at room temperature with 20% animal serum, the type of which was determined by the specific secondary antibody used. Subsequently, the sections were incubated with the primary antibodies (for dilutions see Table 1)

Table 1 Primary antibodies used for IHC, IF and WB analysis (*IHC* immunohistochemistry, *IF* immunofluorescence, *WB* Western blot, *Htau* hyperphosphorylated tau, *LIF* leukemia inhibitory factor, *IGFBP-3* insulin-like growth factor binding protein 3, *Egr-1* early growth response factor-1)

Antigen	Species raised in:	Dilution IHC	Dilution IF	Dilution WB	Source
Aβ (6C6)	Mouse	1:40,000	1:4,000	–	Elan Pharmaceuticals
Htau (AT8)	Mouse	1:200	1:200	–	Innogenetics
LIF	Goat	1:50	1:50	1:100	Santa Cruz
IGFBP-3	Goat	1:600	1:300	1:100	Santa Cruz
Egr-1	Rabbit	1:400	1:200	–	Santa Cruz

overnight at 4°C, followed by an incubation with the appropriate biotin-labeled secondary antibody, at a dilution of 1:200 for 1 h at room temperature. Then, sections were incubated for 1 h with a 1:100 dilution of peroxidase-conjugated avidin-biotin complex (ABC) according to the manufacturer's description. Staining was performed for 10 min with 0.5 mg/ml diaminobenzidine (DAB) as chromogen in PBS with 0.25% H_2O_2 and stopped in tap water. The DAB staining was enhanced with Cu_2SO_4, followed by counterstaining with hematoxylin for 3 min, and then washed thoroughly with tap water for 10 min. After dehydration in 96% alcohol and xylol, sections were enclosed in Permount (Vector). Each incubation step was followed by extensive washing with PBS. All antibody dilutions were in PBS containing 0.1% BSA (PBS/0.1% BSA), which also served as a negative control.

Immunofluorescence staining of human brain cryosections and Aβ-treated HBP

Air-dried sections from frozen tissue (5 µm thick) were fixed in acetone for 10 min. For double staining, sections were simultaneously incubated with the two primary antibodies overnight at 4°C, followed by an incubation with swine anti-rabbit-FITC (dilution 1:80) or sheep anti-mouse-FITC (dilution 1:200) (depending on the first antibody used) and the appropriate biotin-labeled antibody (dilution 1:200) for 45 min at room temperature. Subsequently, the sections were incubated with Texas Red-labeled avidin (dilution 1:500, Vector) for 45 min at room temperature and mounted in Vectashield (Vector). Antibodies were diluted in PBS/0.1% BSA and each incubation step was followed by extensive washing with PBS. The immunofluorescence staining was examined using a confocal laser scanning microscope (Leica, Wetzlar, Germany).

HBP were cultured in eight-well chamber slides (as described above), and incubated with or without $DA\beta_{1–40}$ for 3 days. Thereafter, the cells were fixed with periodate-lysine-paraformaldehyde (PLP) for 10 min and immunofluorescence staining, as described above, was performed. Nuclei were stained with To-Pro-3 (Molecular probes, Eugene, Ore., dilution 1:1,000).

Western blot analysis

HBP were incubated with $DA\beta_{1–40}$ for 3 days as described above, after which supernatant was collected. Cells were washed once with PBS and then solubilized with lysis buffer (one tablet of Complete, mini Protease Inhibitor Cocktail, Boehringer, Mannheim, Germany, dissolved in 10 ml PBS containing 1% SDS) for 15 min at 37°C. Cell lysates and supernatants were stored at –20°C prior to analysis. Lysates of brain tissue from AD patients as well as control patients were obtained by solubilization of 20 cryosections (10 µm each) in lysis buffer for 15 min at 37°C. Aliquots of the lysates and supernatants were diluted 1:1 with dithiothreitol (DTT)-reducing sample buffer and separated on a 12% SDS-polyacrylamide gel. Subsequently, proteins were electrophoretically transferred to a nitrocellulose membrane (Schleicher and Schuell, Dassel, Germany) in blot buffer (250 mM TRIS-glycine, 20% methanol). Unoccupied sites on the membrane were blocked with 5% non-fat milk containing 1:400 20% NaN_3 in PBS containing 0.5% Tween 20 for 2 h at room temperature. Blots were incubated overnight with the primary antibody (for dilutions see Table 1) and then with donkey anti-goat-peroxidase (dilution 1:50,000) or sheep anti-mouse-peroxidase (1:2,000) depending on the type of primary antibody used, for 1 h at room temperature. Controls for nonspecific binding of secondary antibodies revealed no signals. Peroxidase activity was detected using chemiluminescence, according to the manufacturer's protocol (Boehringer, Mannheim, Germany) and exposure to Kodak X-Omat S films.

Results

$DA\beta_{1–40}$ induces degeneration of HBP

Cultured HBP were incubated with 25 µM $DA\beta_{1–40}$. After 3 days of incubation the first signs of cellular degeneration were observed. Cell contours started to disappear, indicating that plasma membranes were disrupted, but all cell bodies remained attached to the culture dish (data not shown). After a prolonged incubation of 6–7 days about 80% of the cells had died [31], whereas in the absence of $DA\beta_{1–40}$ only approximately 2–5% of the cells are not viable, the living cells remaining viable for several weeks. Differential gene expression of a selected number of genes between HBP, incubated with or without $DA\beta_{1–40}$, was compared after a 3-day period, before the occurrence of actual cell death.

Selection of genes for further investigation

The results of the comparative cDNA expression array were determined by visual inspection. Out of the 25 genes showing differences in mRNA expression levels, those with potential involvement in either cell survival or cell death were selected: LIF, IGFBP-3, and Egr-1. mRNA expression levels of these genes in untreated and $DA\beta_{1–40}$-treated HBP are shown in Fig. 1. An increase in gene expression was observed for LIF and IGFBP-3 after incubation with $DA\beta_{1–40}$, whereas a decrease was found for Egr-1.

Immunocytochemistry

LIF expression in cultured HBP

Immunofluorescence staining of cultured HBP showed a filamentous staining of LIF throughout the whole cell body, suggesting a cytoskeleton-like distribution. An increase in expression was observed after incubation with $DA\beta_{1–40}$. Furthermore, LIF expression followed the same

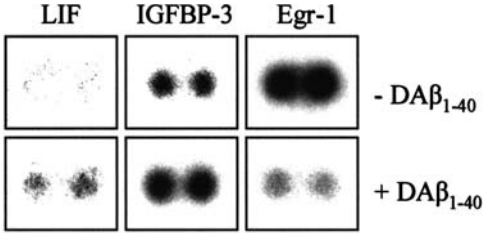

Fig. 1 Differential gene expression of LIF, IGFBP-3 and Egr-1. *Upper panels* represent mRNA levels of untreated HBP, the *lower panels* of HBP treated with $DA\beta_{1–40}$. cDNA is spotted in duplicate. Egr-1 mRNA expression is strongly decreased, LIF and IGFBP-3 mRNA expression levels are increased upon $DA\beta_{1–40}$ treatment (*LIF* leukemia inhibitory factor, *IGFBP-3* insulin-like growth factor binding protein 3, *Egr-1* early growth response factor-1, *HBP* human brain pericyte, *$DA\beta_{1–40}$* amyloid-β carrying the "Dutch" mutation)

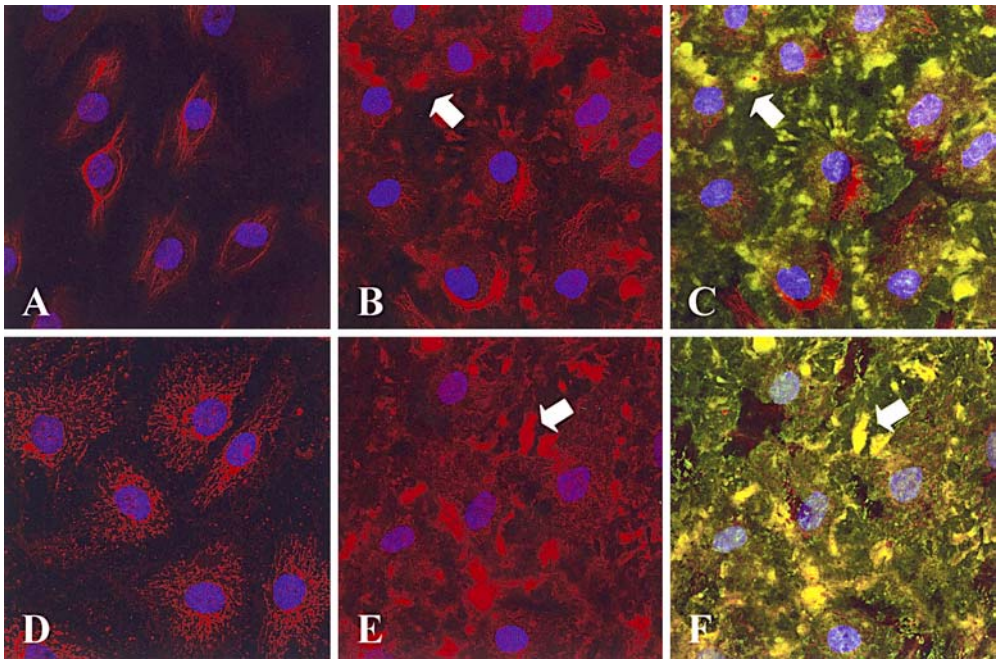

Fig. 2 Immunofluorescence double staining of cultured HBP for Aβ (6C6, monoclonal antibody, *green*) (**C**, **F**) and LIF (polyclonal antibody, *red*) (**A–C**) or IGFBP-3 (polyclonal antibody, *red*) (**D–F**) after 3-day incubation with or without $DA\beta_{1-40}$. **A**, **D** HBP incubated without $DA\beta_{1-40}$ and **B**, **C**, **E**, **F** with $DA\beta_{1-40}$. Nuclei are stained *blue*. *White arrows* indicate examples of co-localization of LIF or IGFBP-3 and Aβ. ×630

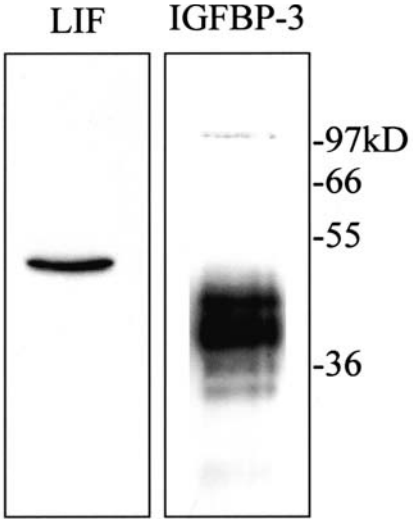

Fig. 3 Western blot of LIF and IGFBP-3 in lysates of cultured HBP. Sizes of molecular weight markers are indicated on the right in kDa.

expression pattern as the supplemented Aβ, suggesting a co-localization of both proteins (Fig. 2A–C, white arrow). LIF expression in HBP was also investigated using Western blotting. One band was observed at approximately 50 kDa, but no consistent differences were observed between HBP incubated with or without $DA\beta_{1-40}$ (Fig. 3, lane 1).

IGFBP-3 expression in cultured HBP

Immunofluorescence staining of IGFBP-3 revealed a granular cytoplasmic localization in cultured HBP. IGFBP-3 staining was increased after incubation of HBP with $DA\beta_{1-40}$ for 3 days. Moreover, IGFBP-3 expression showed a comparable expression pattern as the added $DA\beta_{1-40}$, suggesting an extracellular co-localization (Fig. 2D–F, white arrow). Several bands were observed at molecular masses ranging from approximately 30 to 50 kDa, and one band at nearly 100 kDa (Fig. 3, lane 2). However, again no consistent differences were observed between HBP treated with or without $DA\beta_{1-40}$.

Egr-1 expression in cultured HBP

In HBP, Egr-1 was predominantly expressed in a peri-nuclear location, resembling staining of the Golgi complex (not shown). No differences in expression were observed between $DA\beta_{1-40}$-treated and non-treated HBP. Egr-1 expression could not be detected by Western blotting.

Immunohistochemistry

Aβ and hyperphosphorylated tau

In the brains of all AD patients except one, diffuse as well as classic SPs (Fig. 4A) and neurofibrillary tangles (NFTs; Fig. 4G) were observed. The remaining AD case was characterized by extensive CAA, but neither SPs nor NFTs were observed in the cortex, although classical SPs and NFTs did occur in the hippocampus. CAA was observed in seven AD patients (Fig. 4D). Diffuse SPs were observed in the brains of two control patients, but NFTs were absent.

LIF expression in control and AD brains

In all cases, both control and AD, LIF expression was observed in the cytoplasm of large neurons in the cortex and

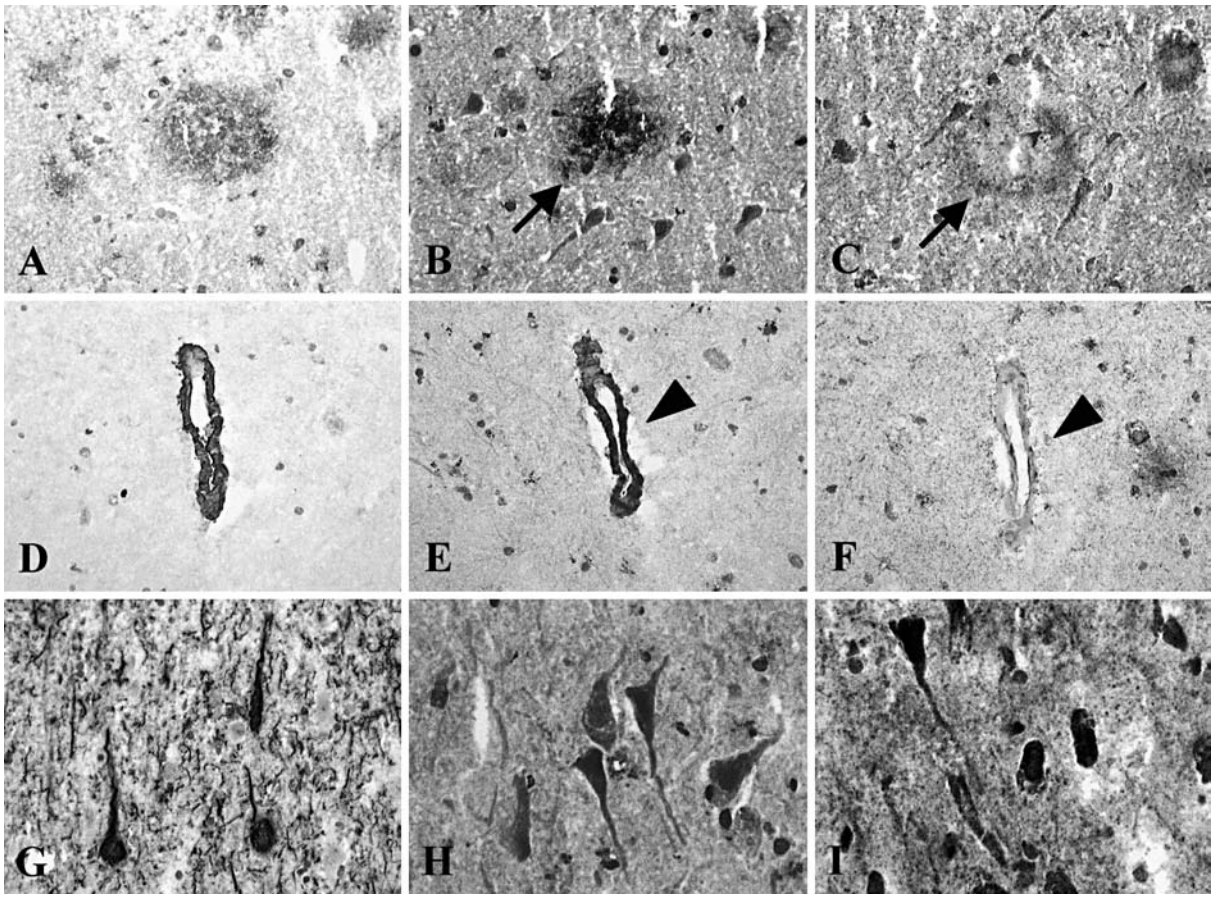

Fig. 4 Immunohistochemical staining of an SP (*black arrow*) in serial sections from AD cortex for Aβ (**A**), LIF (**B**), and IGFBP-3 (**C**). An Aβ-laden vessel (*arrowhead*) is stained in serial sections from AD cortex for Aβ (**D**), LIF (**E**), and IGFBP-3 (**F**). Staining of neurons (random sections) from AD cortex for hyperphosphorylated tau (**G**), LIF (**H**), and IGFBP-3 (**I**) (*AD* Alzheimer's disease, *SP* senile plaque). **A–F** ×250, **G–I** ×400

hippocampus (Fig. 4H). Moreover, in the AD cases, LIF was also expressed in NFTs. Immunofluorescence staining confirmed the co-localization of LIF with hyperphosphorylated tau (Fig. 5G–I). This indicates that LIF is expressed in both unaffected neurons and neurons that contain paired helical filaments of hyperphosphorylated tau. LIF expression could not be observed in unaffected vessels in cortex and hippocampus. In all AD cases and in two control cases, LIF expression was observed in plaques in the cortex and hippocampus (Fig. 4B). If Aβ-laden vessels were present, positive LIF staining could also be detected in these vessels (Fig. 4E). In only one AD case was CAA-associated LIF-expression absent. Co-localization of LIF with SPs and CAA was confirmed in both the cortical and the hippocampal region by immunofluorescence double staining (Fig. 5A–F). Approximately 50–100% of the SPs and 50–100% of the Aβ-laden vessels were positive for LIF.

The results of the semiquantitative examination of the immunohistochemical staining for LIF, IGFBP-3 in AD and control brains are summarized in Table 2.

IGFBP-3 expression in control and AD-brains

Similar to LIF, IGFBP-3 expression was observed in the cytoplasm of large neurons and, in AD-cases, also in NFTs (Fig. 4I). Immunofluorescence double staining confirmed the expression of IGFBP-3 in NFTs (data not shown, but staining was comparable to immunofluorescence staining of LIF as shown in Fig. 5). IGFBP-3 expression was not observed in pericytes in the cortex and hippocampus. IGFBP-3 was expressed in SPs in the cortex of 6 out of 13 AD cases (Fig. 4C) and in 3 AD cases staining was observed in CAA. However, only a fraction (0–50%) of SPs and Aβ-positive vessels were stained for IGFBP-3 (Fig. 4F, example of a vessel affected by CAA but not stained for IGFBP-3). Again, co-localization of IGFBP-3 with Aβ in SPs and CAA was confirmed by immunofluorescence double staining (data not shown). In the hippocampus, IGFBP-3 expression in SPs and CAA was absent.

Egr-1 expression in control and AD brain

Egr-1 expression was observed in astrocytes (Fig. 6), but there was no difference in expression between AD and the control group in both the cortex and hippocampus. Staining for Egr-1 was absent in the characteristic lesions of AD, as confirmed by immunofluorescence double staining (Fig. 5J–L). Furthermore, Egr-1 expression was not al-

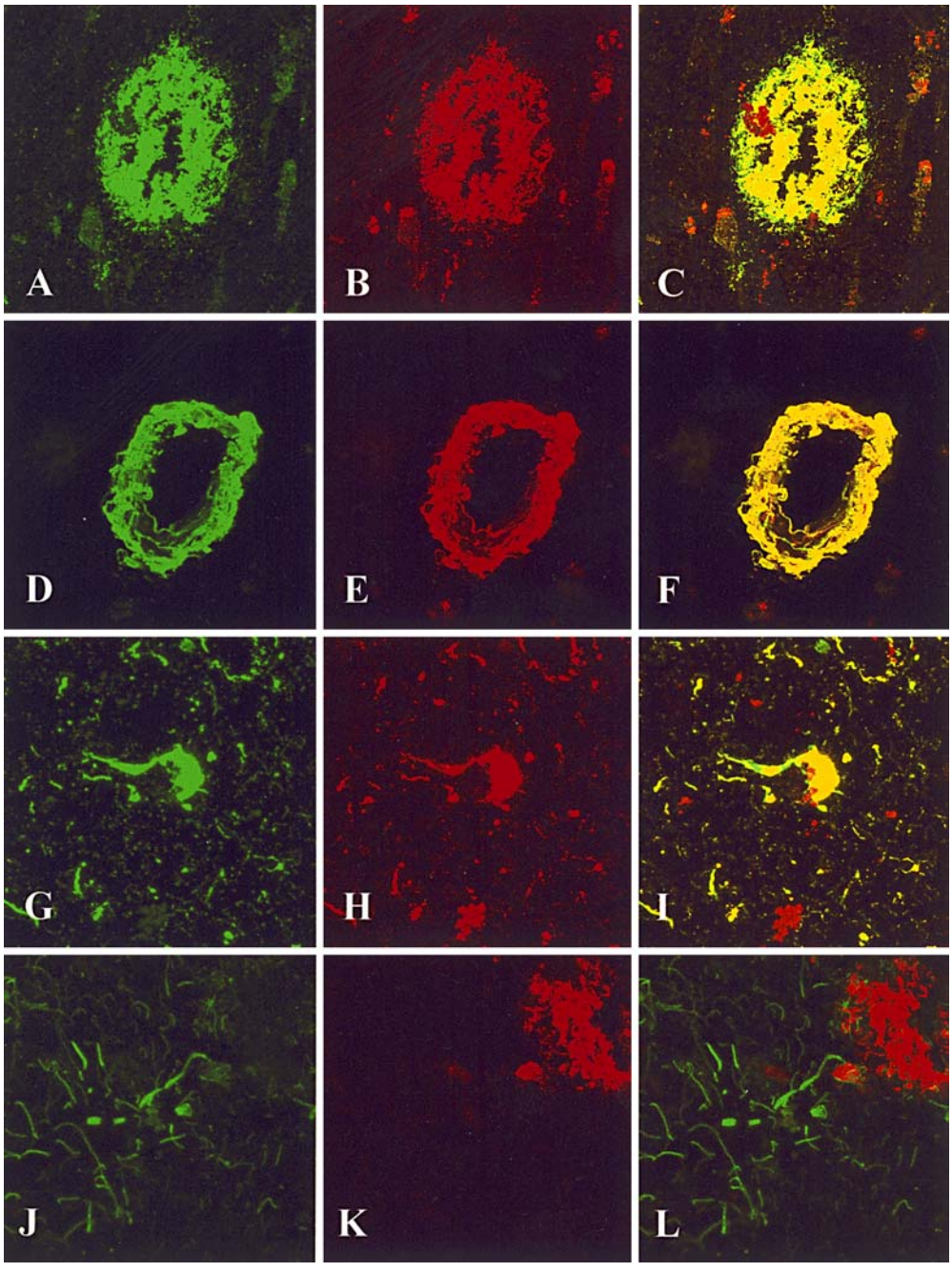

Fig. 5 Immunofluorescence staining of an SP (**A**–**C**) and CAA (**D**–**F**) for both Aβ (*green*) and LIF (*red*). NTFs (**G**–**I**) are stained for both hyperphosphorylated tau (*green*) and LIF (*red*) in AD cortex. Staining for both Egr-1 (*green*) and Aβ (*red*) in AD cortex (**J**–**L**). The *panels* on the *right* show the results of the double staining. LIF co-localized with SPs, CAA and NFTs. Egr-1 did not co-localize with SP or NFTs (*CAA* cerebral amyloid angiopathy, *NFT* neurofibrillary tangle). **A**–**L** ×630

Table 2 Expression of LIF and IGFBP-3 in cortex and hippocampus. Positive fractions (% of senile plaques or CAA-effected vessels stained by a specific antibody compared with Aβ-positive staining) were scored in the following categories: 0% (–), 0–50% (+), 50–100% (++), or 100% (+++). The number of cases with senile plaques or CAA (x) that are positively stained for either LIF or IGFBP-3 (y) is also indicated as a ratio (y/x) (*CAA* cerebral amyloid angiopathy)

		Senile plaques				CAA			
		Cortex		Hippocampus		Cortex		Hippocampus	
AD	LIF	+/++	12/13	+/++	8/11	++/+++	5/7	+/++	4/4
	IGFBP-3	+	6/13	–	0/11	+/++	3/7	–	0/4
Control	LIF	+	2/2	++	1/2	–	0/0	–	0/0
	IGFBP-3	–	0/0	–	0/0	–	0/0	–	0/0

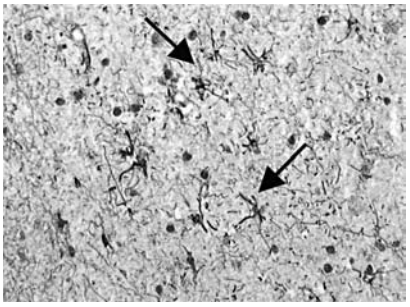

Fig. 6 Immunohistochemical staining of Egr-1 in AD brain, showing that Egr-1 is expressed in astrocytes (*arrow*). ×250

tered in reactive astrocytes surrounding SPs and CAA. Thus, Egr-1 may be a general marker for both nonactivated and activated astrocytes.

Discussion

Aβ is thought to play an important role in the pathogenesis of AD. The toxic properties of Aβ in vitro and in vivo are well established, although the mechanisms of action remain unclear. To uncover some of the effector molecules that mediate Aβ-induced toxicity, a comparative cDNA expression analysis was conducted. Three genes, LIF, IGFBP-3 and Egr-1 were selected for further analysis because of the difference in their mRNA expression levels after Aβ-treatment and their potential role in cell death and survival. The increase in cellular LIF and IGFBP-3 mRNA expression was confirmed on protein level by immunostaining of cultured HBP after incubation with $DA\beta_{1-40}$. Although both LIF and IGFBP-3 could be detected by Western blotting, we could not confirm the increase in protein levels after $DA\beta_{1-40}$ treatment. This may be caused by intimate association of LIF and IGFBP-3 with fibrillar Aβ, leading to reduced solubility. Consequently, in our hands Western blotting appeared to be an unsuitable method to detect differential expression of these proteins in HBP cultures.

No expression of LIF or IGFBP-3 was observed in pericytes in capillaries unaffected by Aβ deposition. However, as discussed previously [30], cross sections of pericytes may be too thin to allow visualization by immunostaining, or HBP may express these proteins only during activation and proliferation, i.e., when they are exposed to culture conditions or in response to Aβ as in the case of CAA.

LIF, and in some cases IGFBP-3, co-localized with vascular Aβ as well as with Aβ in SPs in all AD cases. The cellular origin of either protein remains unclear. Nevertheless, from our in vitro studies, it can be concluded that LIF and IGFBP-3 are produced locally, e.g., by pericytes, SMC or as suggested by other studies, endothelial cells [20]. Accumulation of Aβ in the cerebral vascular wall, eventually leading to CAA, may lead to the degeneration of pericytes and SMC with a concomitant increase in LIF and IGFBP-3 expression by these cells. Although we were unable to visualize the expression of these proteins in pericytes in brain tissue, it is possible that, in Aβ-laden vessels, it is difficult to distinguish the expression of LIF and IGFBP-3 in HBP from their accumulation in CAA. Moreover, both LIF and IGFBP-3 are also expressed by neurons, as suggested by other studies [5, 25], therefore neurons may be the cellular source of these proteins in SPs. Neuronal LIF and IGFBP-3 may be transported by interstitial fluid drainage towards the vasculature [34], leading to its accumulation in Aβ-laden vessels.

The neuropoietic cytokine LIF is related, both in structure and in its mechanism of action, to the interleukin (IL)-6 family of cytokines, which also includes IL-11, ciliary neurotrophic factor (CNTF), oncostatin M, and cardiotrophin [22]. LIF is involved in both neuronal and immune responses to injury [17]. For example, LIF saved sensory, motor, and cholinergic neurons [4] from axotomy-induced cell death and its expression increased in response to peripheral nerve injury [27]. On the other hand, LIF has been described to induce an inflammatory response, e.g., LIF induced expression of both IL-1 and IL-6 [36], and, vice versa, both IL-1 and IL-6 can induce LIF [15]. IL-1 and IL-6 are expressed by activated microglia cells [12] and in SPs in AD brain [1]. In addition, LIF may be a mediator of astrocyte activation [3, 20], a process that is observed in AD brains surrounding SPs. In summary, the increase in LIF expression that is evoked as a response to Aβ-mediated injury in our cell culture model, may also occur in AD brains in an attempt to survive Aβ-induced toxicity. This increased LIF expression may, in turn, generate an inflammatory response [28], which has been described to be tightly associated with SP formation [10] (Fig. 7).

IGFBPs are a complex family of seven closely related proteins that bind to IGFs and thereby act as modulators of IGF availability. Increased expression of IGFBP-3 has been related to the inhibition of cell growth and the induction of apoptosis [2]. IGF-1 may have neurotrophic activity, since it protects and even rescues rat hippocampal primary neurons from Aβ-induced toxicity [9]. The neuroprotective actions of IGF-1 may be inhibited by IGFBP-3, by sequestering IGF-1 from its receptor, and thereby inhibiting cell proliferation and inducing apoptosis [26]. In summary, Aβ-induced expression of IGFBP-3 may lead directly to cell death or to inhibition of cell growth, either by a direct mechanism or indirectly by counteracting the neuroprotective effects of IGF-1. However, given the expression of IGFBP-3 in only a fraction of CAA and SPs, IGFBP-3 seems to play a less prominent role in AD pathogenesis than LIF.

The pleiotrophic immediate early gene Egr-1 appears to be a bifunctional protein that is capable of either the activation or repression of transcription [14]. Egr-1 has been reported to be pro-apoptotic [24] and to be increased after injury [8], but, on the other hand, Egr-1 has also been described as an anti-apoptotic molecule [23]. In this study, we found a clear down-regulation of Egr-1 mRNA levels in HBP incubated with $DA\beta_{1-40}$. However, this was not reflected by a differential expression in AD versus control

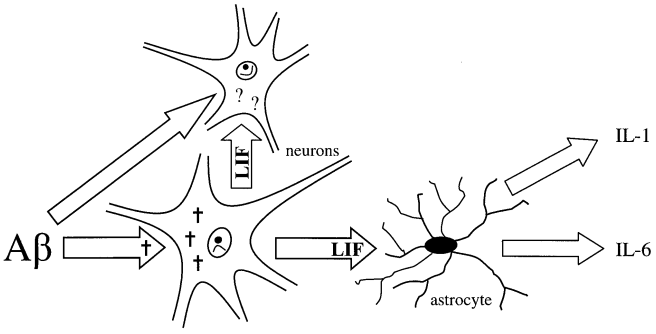

Fig. 7 Schematic presentation of the role of LIF in the pathogenesis of AD. Aβ induces neuronal cellular degeneration and subsequent LIF production. LIF, in turn, may induce activation of astrocytes and microglia, and thereby induce IL-6 production. The production of IL-6 may be followed by an acute phase reaction. On the other hand, LIF is known to protect neurons after injury and may even lead to regeneration of neurons after axotomy. Thus, LIF may also protect neurons against Aβ-induced toxicity

brains. Therefore, the role of Egr-1 in the pathogenesis of AD remains controversial.

In conclusion, the increase in mRNA and protein expression levels in cultured HBP incubated with Aβ suggest that Aβ may also induce excessive LIF production in AD brains, which in turn may be part of an inflammatory response including activation of astrocytes and production of several cytokines such as IL-6 and IL-1 (Fig. 7). On the other hand, LIF may be produced as a response of cells to protect them against Aβ-induced cell death. Aβ may also, albeit to a lesser extent, induce the production of IGFBP-3, which may mediate the cellular degeneration observed in AD brains. Finally, differential gene expression analysis in a culture system can indeed be a useful tool to identify possible mediators involved in SP and CAA formation.

Acknowledgements We thank Dr. Schenk for his kind gift of antibodies. This work was supported by grant 96507 from the 'Internationale Stichting Alzheimer Onderzoek (ISAO)' in The Netherlands.

References

1. Bauer J, Ganter U, Strauss S, Stadtmuller G, Frommberger U, Bauer H, Volk B, Berger M (1992) The participation of interleukin-6 in the pathogenesis of Alzheimer's disease. Res Immunol 143:650–657
2. Buckbinder L, Talbott R, Velasco-Miguel S, Takenaka I, Faha B, Seizinger BR, Kley N (1995) Induction of the growth inhibitor IGF-binding protein 3 by p53. Nature 377:646–649
3. Bugga L, Gadient RA, Kwan K, Stewart CL, Patterson PH (1998) Analysis of neuronal and glial phenotypes in brains of mice deficient in leukemia inhibitory factor. J Neurobiol 36: 509–524
4. Cheema SS, Richards LJ, Murphy M, Bartlett PF (1994) Leukaemia inhibitory factor rescues motoneurones from axotomy-induced cell death. Neuroreport 5:989–992
5. Cheng JG, Patterson PH (1997) LIF is an autocrine factor for sympathic neurons. Mol Cell Neurosci 9:372–380
6. Davis J, Van Nostrand WE (1996) Enhanced pathologic properties of Dutch-type mutant amyloid beta-protein. Proc Natl Acad Sci USA 93:2996–3000
7. Davis-Salinas J, Van Nostrand WE (1995) Amyloid beta-protein aggregation nullifies its pathologic properties in cultured cerebrovascular smooth muscle cells. J Biol Chem 270:20887–20890
8. Dieckgraefe BK, Weems DM (1999) Epithelial injury induces egr-1 and fos expression by a pathway involving protein kinase C and ERK. Am J Physiol 276:G322–G330
9. Dore S, Kar S, Quirion R (1997) Insulin-like growth factor I protects and rescues hippocampal neurons against beta-amyloid- and human amylin-induced toxicity. Proc Natl Acad Sci USA 94:4772–4777
10. Eikelenboom P, Zhan SS, Gool WA van, Allsop D (1994) Inflammatory mechanisms in Alzheimer's disease. Trends Pharmacol Sci 15:447–450
11. Glenner GG, Wong CW (1984) Alzheimer's disease: initial report of the purification and characterization of a novel cerebrovascular amyloid protein. Biochem Biophys Res Commun 120:885–890
12. Griffin WS, Sheng JG, Roberts GW, Mrak RE (1995) Interleukin-1 expression in different plaque types in Alzheimer's disease: significance in plaque evolution. J Neuropathol Exp Neurol 54:276–281
13. Kawai M, Kalaria RN, Cras P, Siedlak SL, Velasco ME, Shelton ER, Chan HW, Greenberg BD, Perry G (1993) Degeneration of vascular muscle cells in cerebral amyloid angiopathy of Alzheimer disease. Brain Res 623:142–146
14. Khachigian LM, Collins T (1998) Early growth response factor 1: a pleiotropic mediator of inducible gene expression. J Mol Med 76:613–616
15. Knight DA, Lydell CP, Zhou D, Weir TD, Robert-Schellenberg R, Bai TR (1999) Leukemia inhibitory factor (LIF) and LIF receptor in human lung. Distribution and regulation of LIF release. Am J Respir Cell Mol Biol 20:834–841
16. Kowall NW, Beal MF, Busciglio J, Duffy LK, Yankner BA (1991) An in vivo model for the neurodegenerative effects of beta amyloid and protection by substance P. Proc Natl Acad Sci USA 88:7247–7251
17. Kurek JB, Radford AJ, Crump DE, Bower JJ, Feeney SJ, Austin L, Byrne E (1998) LIF (AM424), a promising growth factor for the treatment of ALS. J Neurol Sci 160 (Suppl 1): S106–S113
18. Levy E, Carman MD, Fernandez-Madrid IJ, Power MD, Lieberburg I, Van Duinen SG, Bots GT, Luyendijk W, Frangione B (1990) Mutation of the Alzheimer's disease amyloid gene in hereditary cerebral hemorrhage, Dutch type. Science 248:1124–1126
19. Melchor JP, Van Nostrand WE (2000) Fibrillar amyloid beta-protein mediates the pathologic accumulation of its secreted precursor in human cerebrovascular smooth muscle cells. J Biol Chem 275:9782–9791
20. Mi H, Haeberle H, Barres BA (2001) Induction of astrocyte differentiation by endothelial cells. J Neurosci 21:1538–1547
21. Mirra SS, Heyman A, McKeel D, Sumi SM, Crain BJ, Brownlee LM, Vogel FS, Hughes JP, Belle G van, Berg L (1991) The consortium to establish a registry for Alzheimer's disease (CERAD). Part II. Standardization of the neuropathologic assessment of Alzheimer's disease. Neurology 41:479–486
22. Murphy M, Dutton R, Koblar S, Cheema S, Bartlett P (1997) Cytokines which signal through the LIF receptor and their actions in the nervous system. Prog Neurobiol 52:355–378
23. Muthukkumar S, Han SS, Rangnekar VM, Bondada S (1997) Role of Egr-1 gene expression in B cell receptor-induced apoptosis in an immature B cell lymphoma. J Biol Chem 272: 27987–27993
24. Nair P, Muthukkumar S, Sells SF, Han SS, Sukhatme VP, Rangnekar VM (1997) Early growth response-1-dependent apoptosis is mediated by p53. J Biol Chem 272:20131–20138
25. Ocrant I, Fay CT, Parmelee JT (1990) Characterization of insulin-like growth factor binding proteins produced in the rat central nervous system. Endocrinology 127:1260–1267

26. Shen L, Dean NM, Glazer RI (1999) Induction of p53-dependent, insulin-like growth factor-binding protein-3-mediated apoptosis in glioblastoma multiforme cells by a protein kinase Calpha antisense oligonucleotide. Mol Pharmacol 55:396–402
27. Subang MC, Richardson PM (2001) Synthesis of leukemia inhibitory factor in injured peripheral nerves and their cells. Brain Res 900:329–331
28. Sugiura S, Lahav R, Han J, Kou SY, Banner LR, De Pablo F, Patterson PH (2000) Leukaemia inhibitory factor is required for normal inflammatory responses to injury in the peripheral and central nervous systems in vivo and is chemotactic for macrophages in vitro. Eur J Neurosci 12:457–466
29. Van Nostrand WE, Melchor JP, Ruffini L (1998) Pathologic amyloid beta-protein cell surface fibril assembly on cultured human cerebrovascular smooth muscle cells. J Neurochem 70:216–223
30. Verbeek MM, Otte H, I, Wesseling P, Ruiter DJ, De Waal RM (1994) Induction of alpha-smooth muscle actin expression in cultured human brain pericytes by transforming growth factor-beta 1. Am J Pathol 144:372–382
31. Verbeek MM, De Waal RM, Schipper JJ, Van Nostrand WE (1997) Rapid degeneration of cultured human brain pericytes by amyloid beta protein. J Neurochem 68:1135–1141
32. Verbeek MM, Eikelenboom P, De Waal RM (1997) Differences between the pathogenesis of senile plaques and congophilic angiopathy in Alzheimer disease. J Neuropathol Exp Neurol 56:751–761
33. Verbeek MM, Van Nostrand WE, De Waal RMW (2000) Degeneration of human cerebrovascular smooth muscle cells and pericytes caused by amyloid β protein. In: Verbeek MM, De Waal RMW, Vinters HV (eds) Cerebral amyloid angiopathy in Alzheimer's disease and related disorders. Kluwer, Dordrecht, pp 265–279
34. Weller RO, Massey A, Kuo YM, Roher AE (2000) Cerebral amyloid angiopathy: accumulation of A beta in interstitial fluid drainage pathways in Alzheimer's disease. Ann N Y Acad Sci 903:110–117
35. Wisniewski HM, Wegiel J, Wang KC, Lach B (1992) Ultrastructural studies of the cells forming amyloid in the cortical vessel wall in Alzheimer's disease. Acta Neuropathol 84:117–127
36. Zhu M, Oishi K, Lee SC, Patterson PH (2001) Studies using Leukemia inhibitory factor (LIF) knockout mice and a LIF adenoviral vector demonstrate a key anti-inflammatory role for this cytokine in cutaneous inflammation. J Immunol 166:2049–2054